Photomagnetic Properties in a Series of Spin Crossover Compounds $[Fe(PM\text{-}L)_2(NCX)_2]$ (X = S, Se) with Substituted 2′-Pyridylmethylene-4-amino Ligands

Laurence Capes,[a, b] Jean-François Létard,*[a] and Olivier Kahn†[a]

This paper is dedicated to the memory of Olivier Kahn who died on December 8, 1999

Abstract: The spin crossover (SC) compounds $[Fe(PM\text{-}AzA)_2(NCX)_2]$ and $[Fe(PM\text{-}FlA)_2(NCX)_2]$ (with PM-AzA = *N*-2′-pyridylmethylene-4-(phenylazo)aniline, PM-FlA = *N*-2′-pyridylmethylene-4-(2-amino)fluorene, and X = S, Se) have been prepared. The SC regimes have been deduced from variable-temperature magnetic susceptibility data. The enthalpy and entropy changes associated with the SC have been evaluated from DSC measurements. A cooperativity factor, *C*, has been defined, and its values for the different compounds have been deduced from the spin crossover curves. At 10 K, the light-induced excited spin state trapping (LIESST) effect has been observed within the cavity of the SQUID magnetometer. The critical temperatures T_c(LIESST) have been determined for $[Fe(PM\text{-}AzA)_2(NCS)_2]$ and $[Fe(PM\text{-}FlA)_2(NCX)_2]$, and the role of cooperativity has been analyzed. A linear correlation has been found between the T_c(LIESST) and *C* values. The kinetics of HS → LS relaxation have been investigated; a thermally activated mechanism at elevated temperatures and a nearly temperature independent relaxation behavior at low temperatures have been found. Finally, the magnetic behavior recorded under light irradiation in the warming and cooling modes has revealed the occurrence of the light-induced thermal hysteresis (LITH) effect.

Keywords: iron · magnetic properties · photomagnetism · spin crossover

Introduction

High-spin (HS, $^5T_2$) ⇌ low-spin (LS, $^1A_1$) crossovers in iron(II) compounds have been extensively studied during the last two decades. In the solid state, the spin crossover (SC) may be induced by a change of temperature, of pressure, or by light irradiation.[1] The SC occurs when the enthalpy difference between HS and LS states, ΔH_{HL}, is weakly positive. At low temperature, the thermodynamically stable state is the LS state. On the other hand, when the temperature, *T*, is higher than $T_{1/2}$, the HS state becomes the thermodynamically stable state. Indeed, the entropy difference between the two states, ΔS_{HL}, is very large, and $T\Delta S_{HL}$ dominates ΔH_{HL}, so that the Gibbs free energy variation, ΔG_{HL}, becomes negative. $T_{1/2}$ is the inversion temperature for which there is a coexistence of 50% of LS and 50% of HS molecules.[2] While the origin of SC is molecular, the temperature dependence of the HS molar fraction, $\gamma_{HS} = f(T)$, is strongly affected by intermolecular interactions. The stronger these interactions are, the steeper the $\gamma_{HS} = f(T)$ curve around $T_{1/2}$. A model was proposed by Slichter and Drickamer,[3] based on a mean-field approximation, to quantify these intermolecular interactions through an interaction parameter, *Γ*. When *Γ* overcomes a threshold value equal to $2RT_{1/2}$, a bistability domain appears.[4] The temperature of the LS → HS transition in the warming mode, $T_{1/2}\uparrow$, is higher than the temperature of the HS → LS transition in the cooling mode, $T_{1/2}\downarrow$. Between $T_{1/2}\uparrow$ and $T_{1/2}\downarrow$ the system is bistable and its electronic state (LS or HS) depends on its history, and hence on the information that the system stores.

Together with industrial partners, one of us investigated two kinds of displays: rewritable (reversible) and single use displays.[5] It has been proved that SC polymers offer interesting capabilities such as: i) fine tuning of the temperature working range, including room temperature; ii) wide thermal hysteresis loops; iii) short addressing time, and iv) low thermal addressing power. Regarding the last point,

[a] Prof. Dr. J.-F. Létard, L. Capes, Prof. Dr. O. Kahn†
Laboratoire des Sciences Moléculaires
Institut de Chimie de la Matière Condensée de Bordeaux (ICMCB)
UPR CNRS No 9048, 33608 Pessac (France)
Fax: (+33) 556842649
E-mail: letard@icmcb.u-bordeaux.fr

[b] L. Capes
MOTOROLA Centre de Recherche
Espace Technologique Saint Aubin
91193 Gif-sur-Yvette (France)

  0947-6539/00/0612-2246 $ 17.50+.50/0

optical addressing would be an interesting alternative approach. In 1984, Decurtins et al.[6] demonstrated the possibility to convert a LS state into a metastable HS state at 20 K by using a green light irradiation (LIESST effect). Later on, Hauser[7] proved that a red-light switches the system back from the HS to the LS state. This suggests that SC compounds could be used as optical switches. The weak point, however, is that trapping the system in the metastable HS state requires to work at very low temperature. For all the iron(II) spin-crossover compounds exhibiting a LIESST effect, the system clears the energy barrier between the two spin states above a certain temperature, T_c(LIESST),[8, 9] and relaxes to the LS state.

Hauser et al.[10] determined the relaxation rates and the quantum yields of all intersystem-crossing processes involved in the LIESST and reverse-LIESST mechanism. A nearly temperature independent relaxation behavior at low temperatures and a thermally activated relaxation behavior at elevated temperatures were observed. At low temperatures, the dynamics were interpreted on the basis of the non-adiabatic multiphonon relaxation theory.[11] The crucial parameters in this relaxation model are the energy difference, ΔE^0_{HL}, between the lowest vibrational levels of the HS and the LS states and the change of the metal-ligand bond length, Δr_{HL}, that is the relative vertical and horizontal displacements of the two potential wells. In the high-temperature region, the process is thermally activated and strongly influenced by the cooperativity.[12] In pure compounds, the decay curves are non-exponential, whereas in doped mixed crystals single-exponential relaxation curves are observed. The kinetics of the sigmoidal decay in pure (non-doped) SC compounds reflect a self-accelerating relaxation, and the activation energy is a function of the HS molar fraction. Recently, we compared the photomagnetic properties of a series of iron(II) spin-crossover compounds and observed that T_c(LIESST) is governed, at least in part, by the abruptness of the spin transition.[9]

In this paper, we focus on the series of compounds of general formula [Fe(PM-L)$_2$(NCS)$_2$] where PM-L stands for a 2′-pyridylmethylene 4-amino group attached to a L aryl unit (see Figure 1). Despite their chemical similarity, these compounds cover the whole spectrum of SC regimes (see Figure 2): i) [Fe(PM-AzA)$_2$(NCS)$_2$], *cis*-bis(thiocyanato)-bis(*N*-2′-pyridylmethylene)-4-(phenylazo)aniline iron(II), shows a gradual SC with $T_{1/2}$ around 189 K;[13] ii) [Fe(PM-BiA)$_2$(NCS)$_2$], cis-bis(thiocyanato)-bis(*N*-2′-pyridylmethylene)-4-(aminobiphenyl) iron(II), presents two different SC regimes, depending on the synthetic procedure, namely a gradual spin conversion (phase II) around 190 K[14] or an exceptionally abrupt spin transition (phase I) with a very narrow hysteresis ($T_{1/2}\downarrow = 168$ K and $T_{1/2}\uparrow = 173$ K)[8]; iii) finally, [Fe(PM-PEA)$_2$(NCS)$_2$], cis-bis(thiocyanato)bis(*N*-2′-pyridylmethylene)-4-(phenylethynyl) aniline iron(II), presents a very large hysteresis as well as a relatively high transition temperature; for a powder sample, $T_{1/2}\downarrow$ was found as 195 K, and $T_{1/2}\uparrow$ as 255 K.[15]

This series of compounds offers us the opportunity to compare the photomagnetic properties of structurally related materials with different SC regimes. Up to now, only the

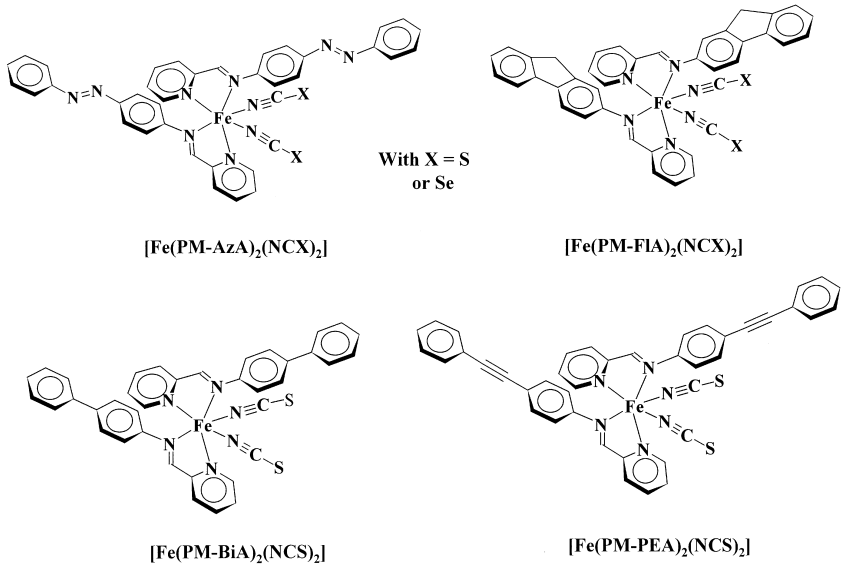

Figure 1. Schematic representation of the [Fe(PM-L)$_2$(NCS)$_2$] compounds.

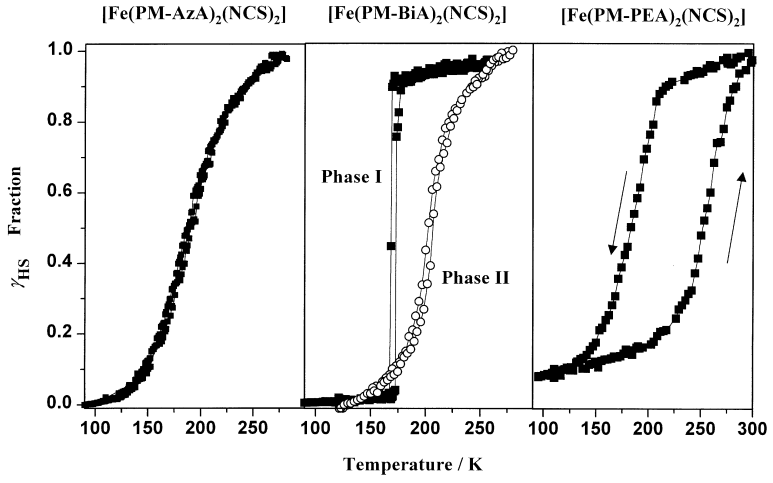

Figure 2. Temperature dependencies of the HS molar fraction for [Fe(PM-AzA)$_2$(NCS)$_2$],[13] [Fe(PM-BiA)$_2$(NCS)$_2$] phase I[8] and phase II,[14] and [Fe(PM-PEA)$_2$(NCS)$_2$] (powder sample).[15]

  0947-6539/00/0612-2247 $ 17.50+.50/0

LIESST properties of $[Fe(PM\text{-}BiA)_2(NCS)_2]$ in phases I and II have been reported.[8, 14] In this paper, we report the synthesis, the magnetic properties, and the LIESST effect of some new members of this $[Fe(PM\text{-}L)_2(NCX)_2]$ family, namely $[Fe(PM\text{-}FlA)_2(NCS)_2]$ with PM-FlA = *N*-2′-pyridylmethylene-4-(2-amino)fluorene, and the selenocyanate derivatives $[Fe(PM\text{-}AzA)_2(NCSe)_2]$ and $[Fe(PM\text{-}FlA)_2(NCSe)_2]$. A special attention will be paid to the influence of cooperativity on the photomagnetic properties, and we will try to define the conditions which must be fulfilled to increase the T_c(LIESST) values in view of designing optical switches. We will also report the LITH (Light-Induced Thermal Hysteresis[8]) experiments carried out on these compounds.

Experimental Section

Syntheses: The $[Fe(PM\text{-}L)_2(NCX)_2]$ (with X = S or Se) compounds were prepared using a stochiometric amount of ligand in order to avoid the problems encountered for $[Fe(PM\text{-}BiA)_2(NCS)_2]$, where two phases were obtained.[8, 14] The Schiff base PM-FlA was synthesized from 2-pyridinecarbaldehyde and 2-aminofluorene.

$[Fe(PM\text{-}FlA)_2(NCS)_2]$ was prepared as follows. Freshly distilled methanol (20 mL), iron(II) sulfate heptahydrate, $FeSO_4 \cdot 7H_2O$ (0.5 g, 1.8 mmol), and potassium thiocyanate, KNCS (0.4 g, 3.7 mmol) were dissolved under nitrogen atmosphere and in the presence of some crystals of ascorbic acid to prevent the iron(II) oxidation. The colorless solution of $Fe(NCS)_2$ was separated from the white precipitate of potassium sulfate by filtration, and added dropwise to a stochiometric amount of PM-FlA ligand in methanol (20 mL). After 1 h a green precipitate of $[Fe(PM\text{-}FlA)_2(NCS)_2]$ was formed. It was filtered off, washed several times with diethyl ether, and dried in a nitrogen stream. Anal. calcd for $FeC_{40}H_{28}N_6S_2$: C 67.42, H 3.93, N 11.80, S 8.99, Fe 7.87; found: C 67.27, H 3.93, N 11.52, S 8.70, Fe 7.79.

Selenocyanate iron(II) compounds were prepared by using KNCSe instead of KNCS. Anal. calcd for $[Fe(PM\text{-}AzA)_2(NCSe)_2]$, $FeC_{38}H_{28}N_{10}Se_2$: C 54.44, H 3.37, N 16.71, Se 18.34, Fe 6.66; found: C 52.77, H 3.24, N 16.11, Se 17.74, Fe 7.04; anal. calcd for $[Fe(PM\text{-}FlA)_2(NCSe)_2]$, $FeC_{40}H_{28}N_6Se_2$: C 59.57, H 3.50, N 10.42, Se 19.58, Fe 6.93; found: C 58.35, H 3.50, N 10.16, Se 18.41, Fe 7.26.

Physical measurements: Elemental analyses were performed by the Service Central d'Analyse (CNRS) in Vernaison, France. The heat capacities were measured with a Perkin–Elmer DSC-7 calorimeter; the cell was cooled at the velocity of 2 K min^{-1}. Magnetic susceptibility measurements were carried out over the temperature range 300–80 K by using a Manics DSM-8 fully automatized Faraday-type magnetometer equipped with a DN-170 Oxford Instruments continuous flow cryostat and a BE 15f Bruker electromagnet operating at about 0.8 T. Data were corrected for the magnetization of the sample holder and diamagnetic contributions.

The LIESST experiments were realized by using a Spectra-Physics series 2025 Kr^+ laser system coupled to the cavity of a MPMS-55 Quantum Design SQUID magnetometer through an optical fiber. The measurements were performed on a very thin layer of powder sample. The weight was estimated by comparing the thermal SC curve with the curve recorded with an heavier and accurately weighed sample. Irradiation was carried out using the multi-line, 647.1 and 676.4 nm, of the Kr^+ laser. The output power on the panel meter was adjusted to 20 mW and the attenuation factor due to the optical setup was estimated to be around 50%.

Results

Magnetic properties and SC regimes: The temperature dependencies of the high-spin molar fraction, γ_{HS}, for $[Fe(PM\text{-}AzA)_2(NCS)_2]$, $[Fe(PM\text{-}BiA)_2(NCS)_2]$, and $[Fe(PM\text{-}PEA)_2(NCS)_2]$ have already been reported and discussed; they are recalled in Figure 2. The results for $[Fe(PM\text{-}AzA)_2(NCSe)_2]$ and $[Fe(PM\text{-}FlA)_2(NCX)_2]$ (with X = S and Se) are shown in Figure 3. For these three novel compounds,

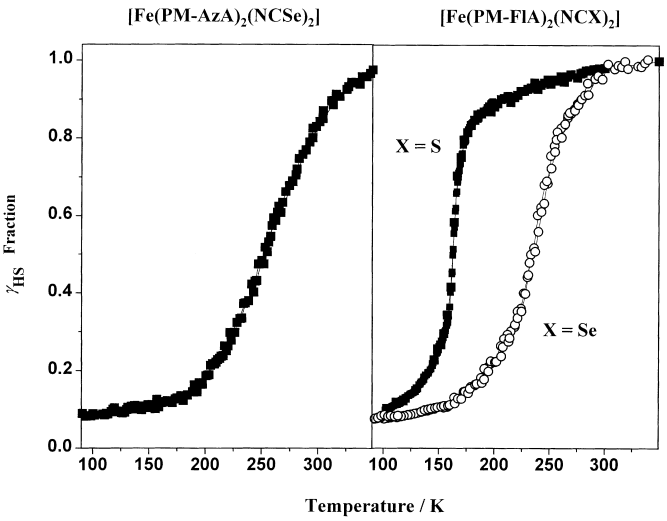

Figure 3. Temperature dependencies of the HS molar fraction for $[Fe(PM\text{-}AzA)_2(NCSe)_2]$ and $[Fe(PM\text{-}FlA)_2(NCX)_2]$ with X = S and Se.

no thermal hysteresis was observed. γ_{HS} at the temperature T is deduced from the molar magnetic susceptibility, χ_M, through Equation (1), where $(\chi_M T)_{HT}$ is the high-temperature limit of $\chi_M T$.

$$\gamma_{HS} = \chi_M T/(\chi_M T)_{HT} \quad (1)$$

The $(\chi_M T)_{HT}$ value is around 3.5 cm^3 K mol^{-1}, which corresponds to what is expected for a spin quintet HS state. This value is reached at about 290 K for the thiocyanate derivatives and 350 K for the selenocyanate derivatives. Let us note that for all the compounds, except $[Fe(PM\text{-}AzA)_2(NCS)_2]$ and $[Fe(PM\text{-}BiA)_2(NCS)_2]$, a residual HS molar fraction at low temperature, f_{HS}, is observed, whose value is around 0.1. The $T_{1/2}$ values for the $[Fe(PM\text{-}L)_2(NCX)_2]$ compounds as well as for some other $[FeN_4(NCX)_2]$ compounds[2, 8, 16–20] are given in the first column of Table 1. A notable increase of $T_{1/2}$ occurs when sulfur is replaced by selenium.

Heat capacity measurements and cooperativity factors: The temperature dependence of the heat capacity was recorded for $[Fe(PM\text{-}FlA)_2(NCX)_2]$ and $[Fe(PM\text{-}AzA)_2(NCX)_2]$. Table 1 collects the values of the enthalpy variation, ΔH_{HL}, and entropy variation, ΔS_{HL}, associated with the SC for the $[Fe(PM\text{-}L)_2(NCX)_2]$ compounds as well as for some other $[FeN_4(NCX)_2]$ compounds.[2, 8, 16–20]

The ΔS_{HL} values in the $[Fe(PM\text{-}L)_2(NCS)_2]$ family increases along the sequence $[Fe(PM\text{-}AzA)_2(NCS)_2] < [Fe(PM\text{-}FlA)_2(NCS)_2] < [Fe(PM\text{-}BiA)_2(NCS)_2]$ (phase I) $\ll [Fe(PM\text{-}PEA)_2(NCS)_2]$. The electronic contributions, ΔS_{el}, are identical for all the compounds, and equal to $R\ln(\Omega_{HS}/\Omega_{LS}) = 13.38$ J K^{-1} mol^{-1}, Ω_{HS} and Ω_{LS} being the spin degeneracies in the HS and LS state, respectively. The contributions due to intramolecular vibrations, $\Delta S_{vib,intra}$, correspond mainly to the changes in Fe–N stretching and N-Fe-N deformation vibra-

0947-6539/00/0612-2248 $ 17.50+.50/0 *Chem. Eur. J.* **2000**, *6*, No. 12

Table 1. Inversion temperature $T_{1/2}$ [K], enthalpy variation ΔH_{HL} [kJ mol^{-1}], entropy variation ΔS_{HL} [J K^{-1} mol^{-1}], and least-squares fitted cooperativity coefficient C (see text).

Compounds[a]	$T_{1/2}$	ΔH_{HL}	ΔS_{HL}	C
[Fe(PM-AzA)$_2$(NCS)$_2$]	189	6.68	35.34	0.48
[Fe(PM-FlA)$_2$(NCS)$_2$]	165	5.19	31.45	1.00
[Fe(PM-FlA)$_2$(NCSe)$_2$]	236	6.68	28.31	0.76
[Fe(PM-BiA)$_2$(NCS)$_2$][b]	168[c]	10.06[c]	59.88[c]	1.16
	173[c]	10.05[c]	58.09[c]	
[Fe(PM-PEA)$_2$(NCS)$_2$]	188	8.86	59.65	1.60
	255		23.02	
[Fe(ptz)$_6$(BF$_4$)$_2$][d]	128.0			
	134.2			
[Fe(phen)$_2$(NCS)$_2$]	176.29[e]	8.60[e]	48.78[e]	1.18
	176.00[f]	7.90[f]	45.40[f]	
[Fe(phen)$_2$(NCSe)$_2$]	231.26[e]	11.60[e]	51.22[e]	0.83
[Fe(abpt)$_2$(NCS)$_2$][g]	180	5.80	33	0.80
[Fe(abpt)$_2$(NCSe)$_2$][g]	224	8.60	38	
[Fe(bt)(NCS)$_2$]$_2$·bypm[h]	171.7	9.54	54.4	
	180.9			
[Fe(bt)(NCSe)$_2$]$_2$·bpym[h]	217.5	9.11	41.5	
	221.4			
[Fe(py)$_2$(phen)(NCS)$_2$]·py	106[i]	3.70[i]	37[i]	0.86

[a] Abpt = 4-amino-3,5-bis(pyridin-2-yl)-1,2,4-triazole, bt = 2,2′-bi-2-thiazoline, bypm = 2,2′-bipyrimidine, phen = phenanthroline, ptz = 1-propyltetrazole, and py = pyridine. [b] Relative to phase I. [c] From ref. [8]. [d] From ref. [16]. [e] Adiabatic calorimetry[2]. [f] From ref. [17]. [g] From ref. [18b]. [h] From ref. [19]. [i] From ref. [20].

tion modes. The crystal structures for [Fe(PM-AzA)$_2$(NCS)$_2$], [Fe(PM-BiA)$_2$(NCS)$_2$] (phase I), and [Fe(PM-PEA)$_2$(NCS)$_2$] were solved in the LS and HS states.[13b] They reveal that the modifications of the FeN_6 cores (bond lengths and angles) between HS and LS states are very similar;[13] therefore, these $\Delta S_{vib,intra}$ contributions may be assumed to be close to each other. If this was the case, the differences in ΔS_{HL} values would reflect the differences in values of the contributions due to intermolecular vibrations, or phonons, $\Delta S_{vib,inter}$. This assumption is in line with the two-dimensional character and the stronger cooperativity for [Fe(PM-BiA)$_2$(NCS)$_2$] and [Fe(PM-PEA)$_2$(NCS)$_2$] with respect to [Fe(PM-AzA)$_2$(NCS)$_2$].[12b]

An estimate of the magnitude of the intermolecular interactions may be obtained, using the mean-field model proposed by Slichter and Drickamer.[3] In this model, the temperature dependence of γ_{HS} is given through the implicit Equation (2):

$$\ln\left(\frac{1-\gamma_{HS}}{\gamma_{HS}-f_{HS}}\right)=\frac{\Delta H_{HL}+\Gamma(f_{HS}+1-2\gamma_{HS})}{RT}-\frac{\Delta S_{HL}}{R} \qquad (2)$$

where Γ is the intermolecular interaction parameter. When Γ is smaller than a threshold value equal to $2RT_{1/2}$, the transition is gradual; for $\Gamma = 2RT_{1/2}$, the transition is abrupt, but without hysteresis; $\Gamma > 2RT_{1/2}$ results in the occurrence of a hysteresis. We will define a cooperativity factor as $C = \Gamma/2RT_{1/2}$. Hysteresis may be observed for $C > 1$. Knowing the ΔH_{HL}, ΔS_{HL}, and f_{HS} values, it is possible to determine the Γ and C values by least-squares fittings of the curves of Figure 2 and Figure 3. Table 1 collects the C values obtained for the compounds of the [Fe(PM-L)$_2$(NCX)$_2$] family and for others iron(II) SC compounds. The cooperativity factor is found to increase along the sequence [Fe(PM-AzA)$_2$(NCS)$_2$] < [Fe(PM-FlA)$_2$(NCS)$_2$] < [Fe(PM-BiA)$_2$(NCS)$_2$] (phase I) < [Fe(PM-PEA)$_2$(NCS)$_2$].

The thermodynamical parameters gathered in Table 1 allow us to analyze the role of the S/Se substitution. ΔH_{HL} is rather insensitive to this S/Se substitution. This is particularly true for [Fe(PM-AzA)$_2$(NCX)$_2$] and [Fe(PM-FlA)$_2$(NCX)$_2$] compounds. In contrast, ΔS_{HL} is significantly affected by the S/Se substitution; it decreases when passing from the thiocyanate to the selenocyanate derivative. It is certainly the $\Delta S_{vib,intra}$ contribution which is the most sensitive to the replacement of sulfur by the much heavier selenium atom at the periphery of the molecule. The shift in $T_{1/2}$ associated with the S/Se substitution may be mainly attributed to an entropy change.

LIESST effect: The LIESST experiments were carried out on powder samples of [Fe(PM-AzA)$_2$(NCX)$_2$], [Fe(PM-FlA)$_2$(NCX)$_2$], and [Fe(PM-PEA)$_2$(NCS)$_2$]. The experimental procedure was the same for all the compounds; this procedure is illustrated in Figure 4 in the case of [Fe(PM-FlA)$_2$(NCS)$_2$]. The compound was first slowly cooled from

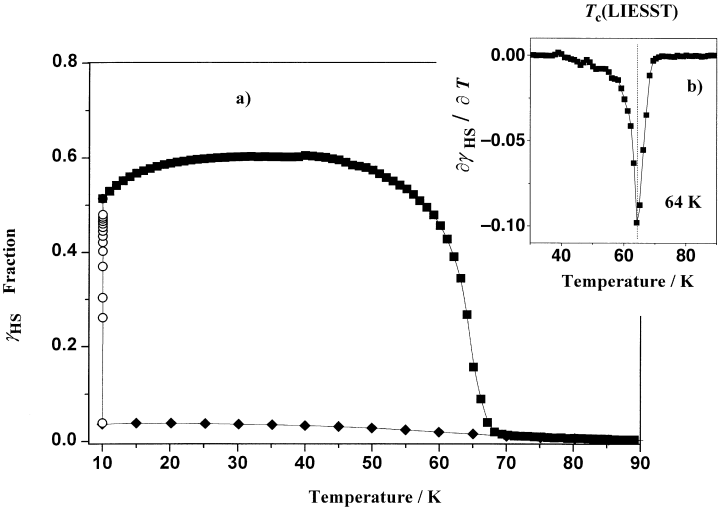

Figure 4. a) Temperature dependence of the photoinduced HS molar fraction for [Fe(PM-FlA)$_2$(NCS)$_2$]: (◆) data recorded in the cooling mode without irradiation; (○) data recorded with irradiation for 1 h at 10 K; (■) data recorded in the warming mode [0.3 K min^{-1}] after the light irradiation was applied for one hour at 10 K, then turned off. b) Derivative $\partial\gamma_{HS}/\partial T$. The extreme of this curve is defined as the T_c(LIESST) value.

about 100 K down to 10 K and the $\chi_M T$ versus T curve was recorded, then transformed into the γ_{HS} versus T curve according to Equation (1). At 10 K, the sample was irradiated for one hour. The magnetic response of the sample increases rapidly before reaching a limiting value, $(\gamma_{HS})_{lim}$. The light irradiation was then turned off, and the temperature was increased at the rate of 0.3 K min^{-1}. $\chi_M T$ (hence γ_{HS}) was found to remain constant when the temperature is low enough, then to drop within a few Kelvin. The critical LIESST temperature, T_c(LIESST),[8, 9] was determined as the extreme of the $\partial\gamma_{HS}/\partial T$ derivative (see Figure 4). The $(\gamma_{HS})_{lim}$ and T_c(LIESST) values for the compounds of the [Fe(PM-L)$_2$(NCX)$_2$] series and for other iron(II) SC compounds recently investigated[9, 18b, 21] in the same way are given in Table 2. No T_c(LIESST) value can be

Table 2. HS molar fraction at 10 K after light irradiation, $(\gamma_{HS})_{lim}$, and experimental, fitted [Eq. (9)] and calculated [Eq. (10)] T_c(LIESST) values [K].

Compounds	$(\gamma_{HS})_{lim}$	T_c(LIESST)		
		Exptl	Fitted	Calcd
$[Fe(PM\text{-}AzA)_2(NCS)_2]$	0.15	31	31	46
$[Fe(PM\text{-}FlA)_2(NCS)_2]$	0.5	64	64	66
$[Fe(PM\text{-}FlA)_2(NCSe)_2]$	0.4	40	40	53
$[Fe(PM\text{-}BiA)_2(NCS)_2]$[e]	0.2	78	75	78
$[Fe(PM\text{-}PEA)_2(NCS)_2]$	≈ 0.05			
$[Fe(ptz)_6(BF_4)_2]$	[a]	60[b]	66	74
$[Fe(phen)_2(NCS)_2]$	0.8	62		
$[Fe(phen)_2(NCSe)_2]$	0.4	47		
$[Fe(abpt)_2(NCS)_2]$	0.3[c]	40[c]	35	38
$[Fe(abpt)_2(NCSe)_2]$	0.3[c]	32[c]		
$[Fe(bt)(NCS)_2]_2 \cdot bypm$[d]	0.3	62		
$[Fe(bt)(NCSe)_2]_2 \cdot bpym$[d]	0.4	46		
$[Fe(py)_2(phen)(NCS)_2] \cdot py$	0.3	47		

[a] The photoinduced magnetic response at 10 K (4.57 $cm^3 K mol^{-1}$), which exceed the value of 3.5 $cm^3 K mol^{-1}$ expected for a HS state has been attributed to orientation effects due to a lamellar structure[6b]. [b] From ref. [9]. [c] From ref. [18b]. [d] From ref. [21]. [e] Relative to phase I[8].

given for $[Fe(PM\text{-}AzA)_2(NCSe)_2]$ and $[Fe(PM\text{-}PEA)_2(NCS)_2]$, as only 5% of HS species are obtained through light irradiation.

The dynamics of the LIESST effect were studied for $[Fe(PM\text{-}AzA)_2(NCS)_2]$ and $[Fe(PM\text{-}FlA)_2(NCX)_2]$ from 6 K up to the highest temperature above which the relaxation becomes too fast for our SQUID setup; these upper-limit temperatures are 45 K, 63 K, and 50 K for $[Fe(PM\text{-}AzA)_2(NCS)_2]$, $[Fe(PM\text{-}FlA)_2(NCS)_2]$ and $[Fe(PM\text{-}FlA)_2(NCSe)_2]$, respectively.

Figure 5 shows the decay of the normalized HS molar fractions, γ_{HS}^N, at 10 K, 30 K, and 50 K. γ_{HS}^N is taken equal to unity at the time $t = 0$ for each temperature. An analysis of these relaxation curves shows a strong deviation from single exponentials. The γ_{HS}^N versus time curves for $[Fe(PM\text{-}AzA)_2(NCS)_2]$ and $[Fe(PM\text{-}FlA)_2(NCSe)_2]$ follow a stretched exponential law at any temperature, while this behavior is observed only at temperatures below 50 K for $[Fe(PM\text{-}FlA)_2(NCS)_2]$; above 50 K, the γ_{HS}^N versus time curves for this compound follow a sigmoidal behavior.

A stretched exponential corresponds to a deviation from a single exponential with a fast initial decay and a long tail with a much slower decay. This behavior was previously reported for iron(II) SC in various environments, such as a powder sample of $[Fe(otz)_6](BF_4)_2$ (otz = 1-*n*-octyltetrazole),[22] a polymer film of $[Fe(mephen)_3]^{2+}$ (2-mephen = 2-methyl-1,10-phenanthroline),[23] and very recently a Langmuir–Blodgett film of $[Fe(Bi\text{-}dfod)_2(NCS)_2]$ (Bi-dfod = 4-(13,13,14,14,15,15,16,16,17,17,18,18,18-tridecafluoroocta-decyl)-4′-methyl-2,2′-bipyridine).[24] This deviation from a single exponential may be attributed to local inhomogeneities of the iron(II) environment or/and to an inhomogeneous photo-excitation due to the attenuation of the penetration of light within the sample. Hauser et al.[23] proposed to analyze the γ_{HS} versus time curves as a distribution of relaxation rates k_{HL} [Eq. (3)], related to a repartition of activation energies. At a given temperature, k_{HL} can be obtained by using a Gaussian distribution of activation energies centered at E_o with a standard deviation of σ and a preexponential factor k_o.

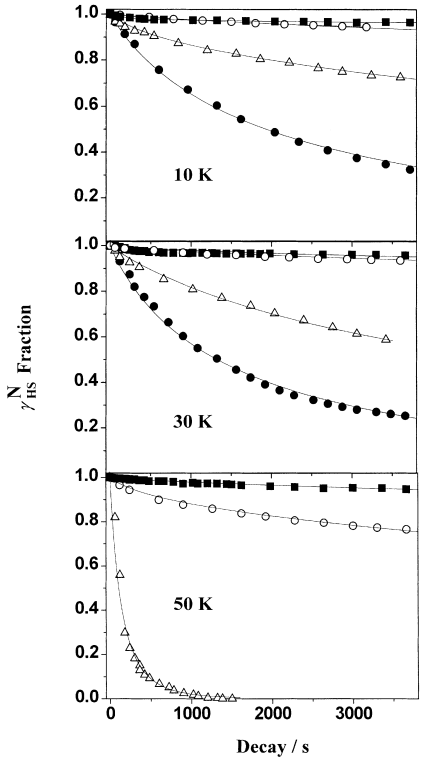

Figure 5. Time dependence at 10, 30, and 50 K of the normalized HS molar fraction (γ_{HS}^N) generated by light irradiation at 10 K for (■) for $[Fe(PM\text{-}BiA)_2(NCS)_2]$ (phase I), (○) for $[Fe(PM\text{-}FlA)_2(NCS)_2]$, (▽) for $[Fe(PM\text{-}FlA)_2(NCSe)_2]$ and (●) for $[Fe(PM\text{-}AzA)_2(NCS)_2]$. γ_{HS}^N corresponds to a normalization at the starting value of the decay for each temperature. The HS → LS relaxation curves follow a stretched exponential and are fitted with Equation (3).

$$\gamma_{HS} = \exp[-k_{HL}t] \quad (3)$$

The k_{HL} values of $[Fe(PM\text{-}L)_2(NCX)_2]$ compounds are reported in Table 3. The γ_{HS}^N versus T curves presented in Figure 5 are fitted with such a distribution of rate constants. At 50 K, the HS → LS relaxation for $[Fe(PM\text{-}AzA)_2(NCS)_2]$ is already too fast to be measured with our SQUID setup.

The sigmoidal behavior encountered for $[Fe(PM\text{-}FlA)_2(NCS)_2]$ between 50 and 63 K was already observed for non-doped compounds exhibiting a cooperative SC.[12b] For diluted SC compounds for which an exponential relaxation is observed, the energy barrier between the HS and LS states, E_a, is constant, and k_{HL} only depends on the temperature. For pure compounds exhibiting cooperative SC, Hauser showed that horizontal and vertical displacements of the two potential wells occur.[12b] This was attributed to an "internal" pressure resulting from the large difference in metal-ligand bond lengths between HS and LS states. The height of the energy barrier is an increasing function of γ_{HS}. At the beginning of the relaxation, γ_{HS} is close to unity; the HS state is stabilized with regard to the LS state. The energy barrier is then large, and the HS → LS relaxation is slow. At the end of the relaxation, γ_{HS} is close to zero; the additional stabilization of the HS state disappears. The energy barrier is small, and a

  0947-6539/00/0612-2250 $ 17.50+.50/0 *Chem. Eur. J.* **2000**, *6*, No. 12

Table 3. Gaussian distribution centered around E_o [cm^{-1}] with a standard deviation σ [cm^{-1}], a preexponential factor k_o [s^{-1}] and a rate constants k_{HL} [s^{-1}] as a function of the temperatures [K] in a series of [Fe(PM-L)$_2$(NCX)$_2$] compounds.

	[Fe(PM-AzA)$_2$(NCS)$_2$]		[Fe(PM-FlA)$_2$(NCS)$_2$]		[Fe(PM-FlA)$_2$(NCSe)$_2$]	
T	σ	k_{HL}	σ	k_{HL}	σ	k_{HL}
6	7	3×10^{-4}	18	5×10^{-8}	10	3×10^{-5}
8	10	3×10^{-4}	25	3×10^{-8}	15	3×10^{-5}
10	10	3×10^{-4}	25	1×10^{-7}	19	4×10^{-5}
15	17	2×10^{-4}	43	4×10^{-8}	25	3×10^{-5}
20	17	3×10^{-4}	50	1×10^{-7}	37	3×10^{-5}
25	18	4×10^{-4}			37	6×10^{-5}
30	27	5×10^{-4}	70	7×10^{-7}	31	1×10^{-4}
35					16	4×10^{-4}
40	43	1×10^{-3}				
42	70	1×10^{-3}				
43	35	5×10^{-3}			37	2×10^{-3}
45	57	1×10^{-2}	105	1×10^{-6}		
46					36	3×10^{-3}
50			101	2×10^{-5}	27	6×10^{-3}

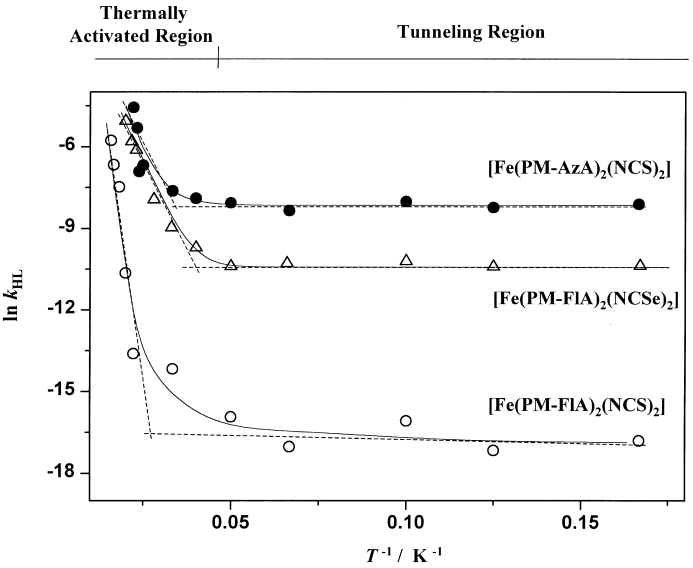

Figure 6. lnk_{HL} versus $1/T$ curve. For $T \geq 20$ K, a straight line is obtained with k_∞^{HT} and E_a^{HT} as thermally activated parameters. For 5 K $< T <$ 20 K, the lnk_{HL} versus $1/T$ plot also gives a straight line with the corresponding tunneling parameters (k_0^{LT}, k_∞^{LT} and E_a^{LT}).

fast relaxation occurs. This can be interpreted as a self-acceleration of the HS → LS relaxation as γ_{HS} decreases. The relaxation rate, k_{HL}^*, then depends on both γ_{HS} and T [Equations (4) and (5)]. The additional activation energy, E_a^*, reflects the cooperativity. In Equation (5), k_{HL} is the preexponential factor which corresponds to the relaxation rate at a given temperature.

$$\frac{\partial\gamma_{HS}}{\partial t} = -k_{HL}^*\,\gamma_{HS} \quad (4)$$

$$k_{HL}^* = k_{HL}\exp\left(\frac{E_a^*}{kT}\gamma_{HS}\right) \quad (5)$$

For [Fe(PM-FlA)$_2$(NCS)$_2$], the γ_{HS}^N versus time curves were fitted with a sigmoidal law at 55, 60, and 63 K. The parameters obtained are 76, 67, and 70 cm^{-1} for E_a^* and 6×10^{-4}, 1×10^{-3}, and 3×10^{-3} s^{-1} for k_{HL}, respectively. The mean additional activation energy, E_a^*, is therefore found to be about 70 ± 6 cm^{-1}. This value can be compared with that of 60 cm^{-1} reported for [Fe(bptn)$_2$(NCS)$_2$] (bptn = 1,7-bis(2-pyridyl)-2,6-diazaheptane),[25] 118 cm^{-1} for [Fe(PM-BiA)$_2$(NCS)$_2$],[8] and 164 cm^{-1} for [Fe(ptz)$_6$(BF$_4$)$_2$].[12a]

From the rate constants k_{HL} obtained with stretched exponential or sigmoidal laws, the activation energy can be calculated from an Arrhenius behavior. Figure 6 shows the lnk_{HL} versus $1/T$ plot for [Fe(PM-AzA)$_2$(NCS)$_2$] and [Fe(PM-FlA)$_2$(NCX)$_2$]. This representation reveals a nearly temperature independent relaxation behavior at low temperatures (LT region) and a thermally activated relaxation behavior at high temperatures (HT region). Then, depending on the temperature range (HT or LT), the activation energy and preexponential factor are defined by Equation (6) with i = HT or LT;

$$k_{HL} = k_\infty^i\exp\left(-\frac{E_a^i}{kT}\right) \quad (6)$$

In the LT region, that is between 6 K and 20 K, the lnk_{HL} versus $1/T$ plot is a straight line (see Figure 6). The activation energies, E_a^{LT}, listed in Table 4 are unusually small, which suggests that tunneling is the predominant mechanism for the relaxation below 20 K. Table 4 also gathers the rate constants as T approaches the absolute zero, named k_0^{LT}. In the theory of nonadiabatic multiphonon relaxation,[11] the low-temperature tunneling rate depends on both the Huang–Rhys factor, S, [Equations (7) and (8)], which is a measure of the horizontal displacement of the potential wells of the HS and LS states, and the energy gap between the lowest vibronic levels of the HS and LS states.

$$k_0^{LT} = \frac{2\pi}{\hbar^2\omega}(\beta_{HL})^2\,\Omega_{LS}\left(\frac{S^p\,e^{-S}}{p!}\right) \quad (7)$$

$$S = \tfrac{1}{2}f\frac{\Delta Q^2}{\hbar\omega} \text{ with } \Delta = \sqrt{6}\Delta r_{HL} \quad (8)$$

where β_{HL} is the electronic tunneling matrix element, $\hbar\omega$ is the frequency of the breathing vibration of the FeN_6 core, $p =$

Table 4. In the tunneling region, E_a^{LT} [cm^{-1}] is the activation energy, k_∞^{LT}[s^{-1}] is the preexponential factor, and k_0^{LT} [s^{-1}] is the rate constant for the HS → LS relaxation as T approaches the absolute zero. In the thermally activated region, E_a^{HT} [cm^{-1}] is the activation energy, E_a^* [cm^{-1}] is the additional activation energy associated with the cooperativity, and k_∞^{HT} [s^{-1}] is the preexponential factor. The term σ [cm^{-1}] corresponds to the standard deviation of the activation energy for stretched exponential relaxation.

	Tunneling region			Thermally activated region		
Compounds	k_∞^{LT}	E_a^{LT}	k_0^{LT}	k_∞^{HT}	$E_a^{HT}(\pm\sigma)$	E_a^*
[Fe(PM-AzA)$_2$(NCS)$_2$]	3×10^{-4}	0.2	3×10^{-4}	9×10^{-2}	100 ± 27	0
[Fe(PM-FlA)$_2$(NCS)$_2$]	6×10^{-8}	0.4	5×10^{-8}	1.7×10^{6}	870	70
[Fe(PM-FlA)$_2$(NCSe)$_2$]	3×10^{-5}	0.2	3×10^{-5}	7	250 ± 30	0
[Fe(PM-BiA)$_2$(NCS)$_2$][a]	4×10^{-6}	0.5	5×10^{-6}	8.7×10^{5}	980	118
[Fe(ptz)$_6$(BF$_4$)$_2$] [12a]				1×10^{5}	797	164
[Fe(abpt)$_2$(NCS)$_2$][18b]	6.6×10^{-4}	7	1×10^{-4}	2	170	0
[Fe(abpt)$_2$(NCSe)$_2$][18b]	2.2×10^{-3}	4	1×10^{-4}			

[a] Relative to the phase I.[8]

$\Delta E^0_{HL}/\hbar\omega$ is the reduced energy gap, and S is the Huang–Rhys factor.

Recently, Hauser et al.[1f] observed a correlation between $\ln k_0^{LT}$ and $T_{1/2}$, assuming a linear dependence between ΔE^0_{HL} and $T_{1/2}$ for a series of FeN_6 SC compounds. Figure 7 shows

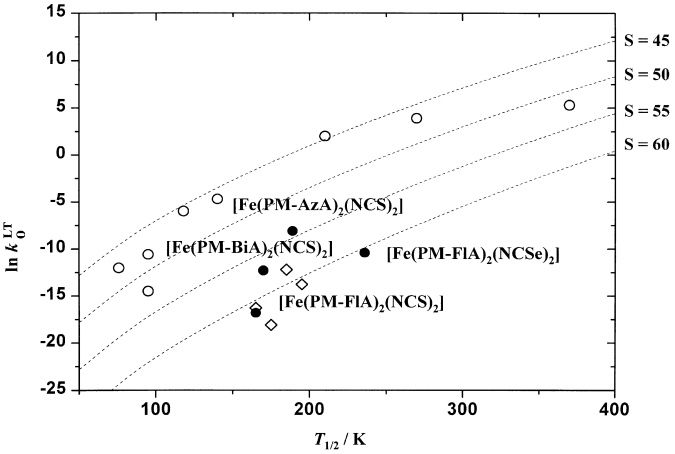

Figure 7. Plot of $\ln k_0^{LT}$ versus $T_{1/2}$ for SC compounds with FeN_6 (○),[1f] FeP_4X_2 (◇) core,[26] and for the $[Fe(PM\text{-}L)_2(NCX)_2]$ compounds (●). The dashed lines are calculated according to Equations (7) and (8), with $\hbar\omega = 250\ cm^{-1}$ and $f = 10^{21}\ cm^{-3}$. The estimated $S = 45$, 50, 55, 60 correspond to an average $\Delta\bar{r}$ of 0.194 Å, 0.205 Å, 0.214 Å, 0.223 Å, respectively.

the $\ln k_0^{LT}$ versus $T_{1/2}$ plots for compounds with FeN_6[1f] or FeP_4X_2[26] cores including our $[Fe(PM\text{-}L)_2(NCX)_2]$ systems. A Huang–Rhys factor close to 55–60 fits reasonably well the $[Fe(PM\text{-}L)_2(NCX)_2]$ data. This situation is probably due to a large change in Fe–N bond lengths [Eq. (8)]. In fact, the crystal structures of $[Fe(PM\text{-}BiA)_2(NCS)_2]$ (phase I) and $[Fe(PM\text{-}AzA)_2(NCS)_2]$ revealed an exceptionally large variation of Fe–N bond lengths, in particular those involving the PM-L ligands, with an average $\Delta\bar{r}$ of 0.218 Å and 0.193 Å, respectively.[13b] From these $\Delta\bar{r}$ values, S factors of 57 and 45, respectively, are expected. A similar observation can be made concerning the compounds with the FeP_4X_2 core;[26] the Fe–P bond lengths vary of 0.27 Å between LS and HS states, with an average $\Delta\bar{r}$ value of 0.2 Å[27].

Correlation between T_c(LIESST) and C: In the thermally activated region ($T > 20$ K), the $\ln k_{HL}$ versus $1/T$ plots for the $[Fe(PM\text{-}L)_2(NCX)_2]$ compounds are straight lines (see Figure 6). The preexponential factors, k_∞^{HT}, and the activation energies barriers, E_a^{HT}, are listed in Table 4. Assuming that T_c(LIESST) is mainly governed by the thermal activation, the values of the parameters listed in Table 4 allow us to simulate the relaxation curves, and to determine theoretically T_c(LIESST). These curves are functions of both time and temperature. From Equations (3)–(6), γ_{HS} in the HT range may be expressed as:

$$\gamma_{HS} = \exp\left[-k_\infty^{HT}\, t\left(-\frac{E_a^{HT} + E_a^*\gamma_{HS}}{kT}\right)\right] \quad (9)$$

With the assumption that γ_{HS} is equal to 0.5 at T_c(LIESST), Equation (10) gives the following expression for T_c(LIESST):

$$T_c(\text{LIESST}) = \frac{E_a^{HT} + E_a^*/2}{k\ln\left[\frac{t\,k_\infty^{HT}}{\ln 2}\right]} \quad (10)$$

Let us suppose, as a first approximation, that only the time at a given temperature is taken into account; t is then equal to 180 s. The calculated T_c(LIESST) values in this approximation are given in Table 2. The agreement between experimental and calculated T_c(LIESST) values is fairly good for strongly cooperative SC compounds; for these compounds, the photoinduced HS fraction changes abruptly within a few Kelvin around T_c(LIESST). Therefore, it is possible to neglect the additional decrease of the HS fraction due to the duration of the experiment.

Let us now take explicitly into account the time factor; Equation (9) in principle allows a simulation of the relaxation curves. Figure 8 compares the experimental and simulated γ_{HS}

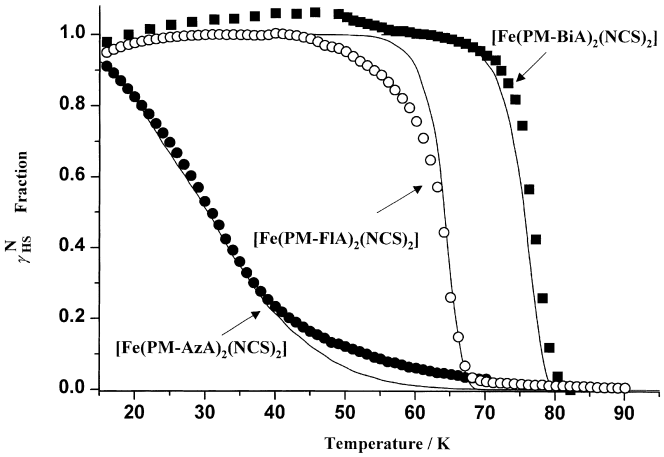

Figure 8. Experimental and simulated temperature dependencies of the normalized HS molar fraction for $[Fe(PM\text{-}AzA)_2(NCS)_2]$, $[Fe(PM\text{-}FlA)_2(NCS)_2]$, and $[Fe(PM\text{-}BiA)_2(NCS)_2]$ (phase I). The simulated curves are in full lines [see text and Equation(9)].

versus T curves for $[Fe(PM\text{-}FlA)_2(NCS)_2]$, $[Fe(PM\text{-}BiA)_2(NCS)_2]$, and $[Fe(PM\text{-}AzA)_2(NCS)_2]$ by using the k_∞^{HT}, E_a^{HT}, and E_a^* parameters of Table 4. The simulated T_c(LIESST) values are given in Table 2. For $[Fe(PM\text{-}FlA)_2(NCS)_2]$ and $[Fe(PM\text{-}BiA)_2(NCS)_2]$ compounds, the agreement is quite satisfying. In the case of $[Fe(PM\text{-}AzA)_2(NCS)_2]$, only an analysis with a Gaussian distribution of E_a^{HT} (100 cm^{-1}) with a standard deviation of 27 cm^{-1} and a preexponential factor of $9.10^{-2}\ s^{-1}$ gives a simulated curve in agreement with the experimental one.

The expression of T_c(LIESST) in Equation (10) suggests that one way to stabilize the photoinduced HS state is to maximize the intermolecular interactions. Along this line, Figure 9 shows the variation of T_c(LIESST) as a function of the cooperativy factor C. A very interesting linear correlation is observed.

LITH effect: Figure 10 presents the photomagnetic behavior for $[Fe(PM\text{-}L)_2(NCS)_2]$ as the light is maintained during both the warming and cooling of the sample. The γ_{HS} versus T plot in the warming mode is rather similar to what is observed

0947-6539/00/0612-2252 $ 17.50+.50/0 Chem. Eur. J. 2000, 6, No. 12

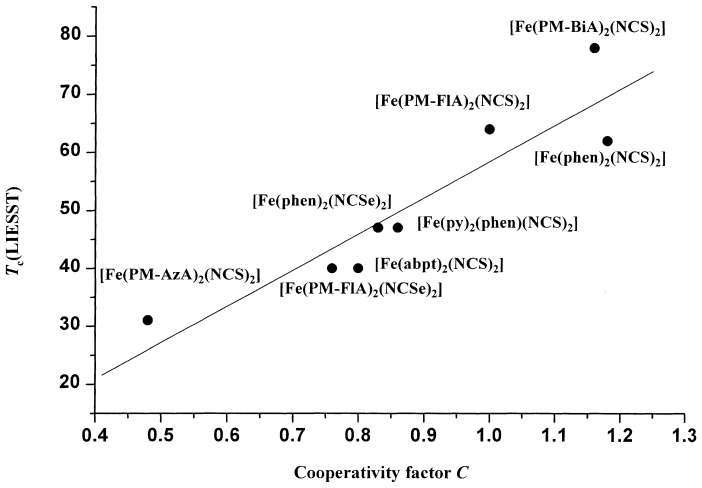

Figure 9. Experimental T_c(LIESST) values (Table 2) as a function of the cooperative factor C for the spin crossover compounds listed in Table 1. The full line is the result of a linear regression.

when the light irradiation is switched off after the generation of the HS species at low temperature (see Figure 8). The γ_{HS} versus T curves in the warming and cooling modes are not identical, the latter being lower than the former. Under irradiation, thermal hysteresis loops are obtained; the light induced thermal hysteresis (LITH) effect reported for the first time by us[8] is observed. The occurrence of the LITH effect was further confirmed by magnetic measurements under irradiation as a function of time (see Figure 10). After

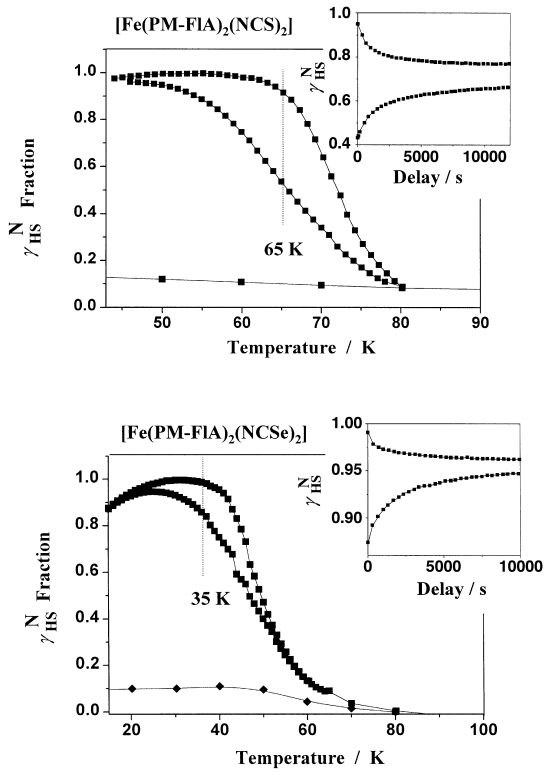

Figure 10. Temperature dependencies of the normalized HS molar fraction obtained after one hour of irradiation at 10 K, then keeping the irradiation both in the warming and cooling modes for [Fe(PM-FlA)$_2$(NCS)$_2$] and [Fe(PM-FlA)$_2$(NCSe)$_2$]. The photo-stationary limit reached for the two compounds in warming and cooling modes (see text) are shown in right graph.

irradiation at 10 K during one hour, the temperature was slowly increased up to 65 K for [Fe(PM-FlA)$_2$(NCS)$_2$] and 35 K for [Fe(PM-FlA)$_2$(NCSe)$_2$]. Then, the temperature was kept constant for nearly 3 h and the magnetic response recorded until a photostationary state was reached. The sample was then warmed up to 99 K without further irradiation, in order to erase the HS information. From this point, the temperature was slowly lowered, and adjusted to 65 K for [Fe(PM-FlA)$_2$(NCS)$_2$] and 35 K [Fe(PM-FlA)$_2$(NCSe)$_2$]. The temperature was kept constant for 3 h and the magnetic response recorded under irradiation. A new photostationary point was then reached. For each compound, the two photostationary points, in the warming and cooling modes, are different. This type of photoinduced bistability was recently reported for [Fe(PM-BiA)$_2$(NCS)$_2$],[8] [Fe$_x$Co$_{1-x}$(btr)$_2$(NCS)$_2$]·H$_2$O, with $x = 0.3$, 0.5, 0.85[28] and [Fe(abpt)$_2$(NCX)$_2$].[18b]

Discussion

The investigation of the photomagnetic properties for iron(II) SC compounds bring new insights on the relaxation processes. Hauser et al.[10] studied a series of doped compounds and demonstrated a correlation between the tunneling rate, $\ln k_0^{LT}$, at low temperatures and $T_{1/2}$ on the basis of the nonadiabatic multiphonon theory.[11] Recently, we reported the T_c(LIESST) values for 22 compounds; T_c(LIESST) was found to increase as $T_{1/2}$ decreases and as the cooperativity increases.[9] In this work, we first defined the cooperativity factor, C, for a SC compound as the ratio $\Gamma/2RT_{1/2}$, where Γ is the interaction parameter in the Slichter and Drikamer model.[3] Then, we determined the C values for a series of [Fe(PM-L)$_2$(NCX)$_2$] compounds from magnetic data (Table 1). For the thiocyanate derivatives, the cooperativity increases as: [Fe(PM-AzA)$_2$(NCS)$_2$] < [Fe(PM-FlA)$_2$(NCS)$_2$] < [Fe(PM-BiA)$_2$(NCS)$_2$] (phase I).

The main part of this work is devoted to the study of the photomagnetic properties. The relaxations from the photoinduced HS state to the LS state were investigated. The abruptness of the γ_{HS} versus T relaxation curves varies as [Fe(PM-AzA)$_2$(NCS)$_2$] < [Fe(PM-FlA)$_2$(NCS)$_2$] < [Fe(PM-BiA)$_2$(NCS)$_2$] (Phase I). This sequence is the same as that found for the cooperativity.

The role of cooperativity is also reflected in the dynamics of the HS → LS relaxation. A non-exponential behavior governed by a Gaussian distribution of activation energies is observed for [Fe(PM-AzA)$_2$(NCS)$_2$] which exhibits a gradual SC. On the other hand, the relaxation process follows a sigmoidal law for [Fe(PM-FlA)$_2$(NCS)$_2$] and [Fe(PM-BiA)$_2$(NCS)$_2$] which exhibit more cooperative SC behaviors. The additional energy activation, E_a^*, increases in the same way as the cooperativity factor, C.

An expression for T_c(LIESST) has been derived [Eq. (10)]. This expression reveals that T_c(LIESST) increases as E_a^* (hence C) increases, which agrees with the experimental observations. As a matter of fact, the extremely abrupt thermal SC presented by [Fe(PM-BiA)$_2$(NCS)$_2$] is associated with one to the highest T_c(LIESST) values recorded to date,

78 K.[8, 9] Unfortunately, the approach consisting in enhancing further the cooperativity in order to increase T_c(LIESST) has some limitations. The most cooperative compound of the $[Fe(PM\text{-}L)_2(NCS)_2]$ series is $[Fe(PM\text{-}PEA)_2(NCS)_2]$. For this compound, only 5% of the metastable HS state can be populated under light irradiation at low temperature. The photostationary limits reached under light irradiation, $(\gamma_{HS})_{lim}$, are listed in Table 2; $(\gamma_{HS})_{lim}$ values much below the unity may have different origins, namely: i) The opacity of the sample may prevent the penetration of light, and inhomogeneous effects may be observed. If it is so, the photomagnetic effect mainly occurs at the surface of the sample, while the SQUID detection is relative to the bulk; ii) The photostationary point reached at 10 K may correspond to an equilibrium between photoinduced population of the HS state and HS → LS relaxation. For most compounds, the lifetime of the HS state at 10 K is very long, and the relaxation is mainly governed by the tunneling effect. However, it cannot be excluded that a compound with a small Δr_{HL} and/or a high ΔE^0_{HL} exhibits a fast relaxation, even at 10 K. iii) The zero field splitting within the HS state may lead to a $\chi_M T$ value which is not proportional anymore to γ_{HS}. iv) Finally, a local heating of the sample during the irradiation might be envisaged. In fact, this heating effect may be ruled out as the magnetic response remains unchanged when the irradiation is turned off. The kinetics of relaxation for all the compounds are very slow at low temperature, except for $[Fe(PM\text{-}AzA)_2(NCS)_2]$. If this compound is excluded of the comparison, the $(\gamma_{HS})_{lim}$ values smaller than unity cannot be attributed to the effect ii). Finally, it can be assumed that the zero field effect iii) is identical for all the compounds. If it is so, $(\gamma_{HS})_{lim}$ seems to be correlated with the cooperativity. More precisely, $(\gamma_{HS})_{lim}$ decreases as C increases. Perhaps, there is a threshold value for C above which the LIESST effect cannot be observed anymore. This would explain why the yield of LIESST is so small for $[Fe(PM\text{-}PEA)_2(NCS)_2]$.

The mechanism of LIESST and reverse-LIESST effects is now well understood.[7, 10] On the other hand, the crystal structure of the photoinduced HS phase remains an open problem. In 1990, Gütlich and co-workers determined the lattice deformations accompanying the thermal and light-induced SC in the case of $[Fe(ptz)_6](BF_4)_2$.[29] The interesting result was that the volume of the unit cell for the "metastable crystal" was halfway between that of the HS phase (above 130 K) and of the LS phase (below 130 K). Another way to obtain some insights on the structure of the photoinduced HS species consists in comparing the relaxation of both thermally and light-induced metastable HS states. Thermally induced metastable HS states may be generated in some cases by rapid cooling of the sample.[30] For $[Fe(bpp)_2](CF_3SO_3)_2 \cdot H_2O$ and $[Fe(bpp)_2](BF_4)_2$, Gütlich and Goodwin[31] found that the rate of the HS → LS relaxation is much faster for HS species generated by LIESST than by rapid cooling. They postulated that a phase transition was necessary in order for the HS → LS relaxation to take place, and therefore the rate of conversion for thermally generated HS states was a measure of the rate of the phase transition. Recently, McGarvey et al.[32] reported a X-band ESR study for the Mn^{2+}-doped $[Fe(bpp)_2](CF_3SO_3)_2 \cdot H_2O$ and $[Fe(bpp)_2](BF_4)_2$ compounds. They followed the variation of the axial zero-field splitting parameter of Mn^{2+}, D, along the thermally induced SC, and found that a phase transition takes place for both compounds. The D values for the HS species generated by a rapid cooling at 77 K were very similar to those observed at room temperature, confirming that a phase transition should take place before the HS → LS transformation begins. In contrast, they found that the photoinduced HS species have the same structure as the LS species; there was no change in X-band EPR spectrum upon irradiation. To sum up, in the case of thermally induced SC accompanied by a crystallographic phase transition, the photoinduced HS species have the same structure neither as the thermodynamically stable HS species, nor as the HS species trapped by rapid cooling.

For a series of iron(II) spin SC compounds, a linear variation of T_c(LIESST) as a function of the cooperativity factor C was found. This result seems to us to be important. It indicates, or at least suggests a relation between photo-induced and thermally induced processes. Perhaps, this linear correlation is valid because the HS species involved in the two processes have the same structure. We already know that the SC for $[Fe(PM\text{-}AzA)_2(NCS)_2]$,[13b] $[Fe(PM\text{-}BiA)_2(NCS)_2]$[8] (Phase I), and $[Fe(Phen)_2(NCS)_2]$[33] occurs without crystallographic phase transition. On the other hand, the crystal structures of the other compounds considered in Figure 9 are still unknown.

Conclusion

The comparison between thermally induced SC and photoinduced HS → LS relaxation provides new information on the LIESST phenomenon. For a series of related SC compounds, the thermal process was first investigated, and the cooperativity factors were determined. The photoinduced process was then studied. An analytical Equation describing quantitatively the HS → LS relaxation, and allowing to determine the T_c(LIESST) values was established. This Equation leads to a very good simulation of the experimental data. Furthermore, it points out the role of cooperativity in the relaxation behavior. A remarkable linear dependence of T_c(LIESST) as a function of C was observed. This result suggests a strategy to increase the temperature range in which the photoinduced information is retained, which consists in increasing the intermolecular interactions. The techniques of supramolecular chemistry allow to work along this line. This strategy, however, has some limitations. The yield of the LIESST effect becomes negligibly small as a SC compound becomes very cooperative.

Acknowledgement

We are grateful for financial support from the European Commission for granting the TMR-Network "Thermal and Optical Switching of Spin States (TOSS)", Contract No. ERB-FMRX-CT98-0199. We would like to thank D. Denux and L. Rabardel (ICMCB, Bordeaux) for the heat capacities measurements.

[1] a) H. A. Goodwin, *Coord. Chem. Rev.* **1976**, *18*, 293–325; b) P. Gütlich, *Struct. Bonding* **1981**, *44*, 83–195; c) H. Toftlund, *Coord.*

  0947-6539/00/0612-2254 $ 17.50+.50/0 *Chem. Eur. J.* **2000**, *6*, No. 12

Chem. Rev. **1989**, *94*, 67–108; d) P. Gütlich, A. Hauser, *Coord. Chem. Rev.* **1990**, *97*, 1–22; e) E. König, *Struct. Bonding* **1991**, *76*, 51–152; f) A. Hauser, *Coord. Chem. Rev.* **1991**, *111*, 275–290; g) P. Gütlich, A. Hauser, H. Spiering, *Angew. Chem.* **1994**, *106*, 2109–2141; *Angew. Chem. Int. Ed. Engl.* **1994**, *33*, 2024–2054; h) P. Gütlich, J. Jung, H. Goodwin, *Molecular Magnetism*: *From Molecular Assemblies to the Devices* (Eds.: E. Coronado, P. Delhaès, D. Gatteschi, J. S. Miller), NATO ASI Series E: Applied Sciences, Vol. 321, Kluwer, Dordrecht, **1996**, pp. 327–378.

[2] M. Sorai, S. Seki, *J. Phys. Chem. Solids* **1974**, *35*, 555–570.

[3] C. P. Slichter, H. G. Drickamer, *J. Chem. Phys.* **1972**, *56*, 2142–2160.

[4] K. F. Purcell, M. P. Edwards, *Inorg. Chem.* **1984**, *23*, 2620–2625.

[5] a) O. Kahn, J. P. Launay, *Chemtronics* **1988**, *3*, 140–151; b) J. Zarembowitch, O. Kahn, *New J. Chem.* **1991**, *15*, 181–190; c) O. Kahn, J. Kröber, C. Jay, *Adv. Mater.* **1992**, *4*, 718–728; d) O. Kahn, *Molecular Magnetism*, VCH, New York, **1993**; e) C. Jay, F. Grollière, O. Kahn, J. Kröber, *Mol. Cryst. Liq. Cryst.* **1993**, *234*, 255–262; f) O. Kahn, C. Jay Martinez, *Science* **1998**, *279*, 44–48; g) Y. Garcia, P. J. van Koningsbruggen, E. Codjovi, R. Lapouyade, O. Kahn, L. Rabardel, *J. Mater. Chem.* **1997**, *7*, 857–858.

[6] a) S. Decurtins, P. Gütlich, C. P. Köhler, H. Spiering, A. Hauser, *Chem. Phys. Lett.* **1984**, *105*, 1–4; b) S. Decurtins, P. Gütlich, K. M. Hasselbach, A. Hauser, H. Spiering, *Inorg. Chem.* **1985**, *24*, 2174–2178.

[7] A. Hauser, *Chem. Phys. Lett.* **1986**, *124*, 543–548.

[8] J.-F. Létard, P. Guionneau, L. Rabardel, J. A. K. Howard, A. E. Goeta, D. Chasseau, O. Kahn, *Inorg. Chem.* **1998**, *37*, 4432–4441.

[9] J.-F. Létard, L. Capes, G. Chastanet, N. Moliner, S. Létard, J. A. Real, O. Kahn, *Chem. Phys. Lett.* **1999**, *313*, 115–120.

[10] A. Hauser, *J. Chem. Phys.* **1991**, *94*, 2741–2748.

[11] E. Buhks, G. Navon, M. Bixon, J. Jortner, *J. Am. Chem. Soc.* **1980**, *102*, 2918–2923.

[12] a) A. Hauser, P. Gütlich, H. Spiering, *Inorg. Chem.* **1986**, *25*, 4245–4248; b) A. Hauser, *Chem. Phys. Lett.* **1992**, *192*, 65–70.

[13] a) V. Ksenofontov, G. Levchenko, H. Spiering, P. Gütlich, J.-F. Létard, Y. Bouhedja, O. Kahn, *Chem. Phys. Lett.* **1998**, *294*, 545–553; b) P. Guionneau, J.-F. Létard, D. S. Yufit, D. Chasseau, G. Bravic, A. E. Goeta, J. A. K. Howard, O. Kahn, *J. Mater. Chem.* **1999**, *9*, 985–994.

[14] a) J.-F. Létard, S. Montant, P. Guionneau, P. Martin, A. Le Calvez, E. Freysz, D. Chasseau, R. Lapouyade, O. Kahn, *Chem. Commun.* **1997**, 745–746; b) J.-F. Létard, H. Daubric, C. Cantin, J. Kliava, Y. A. Bouhedja, O. Nguyen, O. Kahn, *Mol. Cryst. Liq. Cryst.* **1999**, *335*, 495–509.

[15] a) J.-F. Létard, P. Guionneau, E. Codjovi, O. Lavastre, G. Bravic, D. Chasseau, O. Kahn, *J. Am. Chem. Soc.* **1997**, *119*, 10861–10862; b) H. Daubric, C. Cantin, C. Thomas, J. Kliava, J.-F. Létard, O. Kahn, *Chem. Phys.* **1999**, *244*, 75–88.

[16] E. W. Müller, J. Ensling, H. Spiering, P. Gütlich, *Inorg. Chem.* **1983**, *22*, 2074–2078.

[17] J. P. Martin, A. Dworkin, J. Zarembowitch, private communication.

[18] a) N. Moliner, M. C. Muñoz, P. J. Koningsbruggen, J. A. Real, *Inorg. Chim. Acta* **1998**, *274*, 1–6; b) N. Moliner, M. C. Muñoz, S. Létard, J.-F. Létard, X. Solans, R. Burriel, M. Castro, O. Kahn, J. A. Real, *Inorg. Chim. Acta* **1999**, *291*, 279–288.

[19] J. A. Real, I. Castro, A. Bousseksou, M. Verdaguer, B. Burriel, M. Castro, J. Linares, F. Varret, *Inorg. Chem.* **1997**, *36*, 455–464.

[20] R. Claude, J.-A. Real, J. Zarembowitch, O. Kahn, L. Ouahab, D. Grandjean, K. Boukheddaden, F. Varret, A. Dworkin, *Inorg. Chem.* **1990**, *29*, 4442–4448.

[21] J.-F. Létard, J. A. Real, N. Moliner, A. B. Gaspar, L. Capes, O. Cador, O. Kahn, *J. Am. Chem. Soc.* **1999**, *121*, 10630–10631.

[22] T. Buchen, P. Gütlich, *Chem. Phys. Lett.* **1994**, *220*, 262–266.

[23] A. Hauser, J. Adler, P. Gütlich, *Chem. Phys. Lett.* **1988**, *152*, 468–472.

[24] J.-F. Létard, O. Nguyen, H. Soyer, C. Mingotaud, P. Delhaès, O. Kahn, *Inorg. Chem.* **1999**, *38*, 3020–3021.

[25] T. Buchen, H. Toftlund, P. Gütlich, *Chem. Eur. J.* **1996**, *2*, 1129–1133.

[26] C.-C. Wu, J. Jung, P. K. Gantzel, P. Gütlich, D. N. Hendrickson, *Inorg. Chem.* **1997**, *36*, 5339–5347.

[27] F. Cecconi, M. Di Vaira, S. Midollini, A. Orlandini, L. Sacconi, *Inorg. Chem.* **1981**, *20*, 3423–3430.

[28] A. Desaix, O. Roubeau, J. Jeftic, J. G. Haasnoot, K. Boukheddaden, E. Codjovi, J. Linares, M. Nogués, F. Varret, *Eur. Phys. J.* **1998**, *B6*, 183–193.

[29] L. Wiehl, H. Spiering, P. Gütlich, K. Knorr, *J. Appl. Cryst.* **1990**, *23*, 151–160.

[30] G. Ritter, E. König, W. Irler, H. A. Goodwin, *Inorg. Chem.* **1978**, *17*, 224–228.

[31] a) T. Buchen, P. Gütlich, H. A. Goodwin, *Inorg. Chem.* **1994**, *33*, 4573–4576; b) T. Buchen, P. Gütlich, K. H. Sugiyarto, H. A. Goodwin, *Chem. Eur. J.* **1996**, *2*, 1134–1138.

[32] R. C. W. Sung, B. R. McGarvey, *Inorg. Chem.* **1999**, *38*, 3644–3650.

[33] a) B. Gallois, J.-A. Real, C. Hauw, J. Zarembowitch, *Inorg. Chem.* **1990**, *29*, 1152–1158; b) J.-A. Real, B. Gallois, T. Granier, F. Suez-Panamà, J. Zarembowitch, *Inorg. Chem.* **1992**, *31*, 4972–4979.

Received: November 16, 1999 [F2143]